A New Ionic Liquid Electrolyte Enhances the Conversion Efficiency of Dye-Sensitized Solar Cells

Peng Wang, Shaik M. Zakeeruddin,* Jacques-E. Moser, and Michael Grätzel*

Laboratory for Photonics and Interfaces, Institute of Molecular & Biological Chemistry, Ecole Polytechnique Fédérale de Lausanne, CH 1015, Lausanne, Switzerland

Received: June 2, 2003; In Final Form: September 24, 2003

An ionic liquid electrolyte composed of 1-methyl-3-propylimidazolium iodide, 1-methyl-3-ethylimidazolium dicyanamide, and lithium iodide (LiI) was combined with an amphiphilic polypyridyl ruthenium sensitizer to obtain a solar cell based on a solvent-free electrolyte that had an efficiency of 6.6% at an irradiance of air mass 1.5 (AM 1.5, 100 mW cm^{-2}) and >7.1% at lower light intensities. This is the first time such a high efficiency was obtained for dye-sensitized solar cells with pure ionic liquid electrolytes. A thin-layer electrochemical cell was used to determine the redox potential of sensitizers anchored on TiO_2 nanocrystalline film by square-wave voltammetry. Laser transient absorbance measurements revealed that a significant enhancement of the device efficiency, after adding LiI to the ionic liquid electrolyte, could be ascribed to an increase in the electron injection yield and dye regeneration rate.

Introduction

The rapid depletion of fossil fuels and disastrous environmental problems of their combustion are forcing us to develop renewable energy resources for growing energy demands.[1−3] Fortunately, solar energy has a great potential to fulfill an important part of the sustainable energy demand of future generation. During the past decade, dye-sensitized solar cells (DSCs) have attracted much attention as low-cost alternatives to conventional inorganic photovoltaic devices.[4−7] The mesoscopic TiO_2 film texture in these cells significantly increases the cross section for surface-anchored light harvesters while maintaining a good contact with electrolytes. In these devices, photon-to-electricity conversion is achieved by ultrafast electron injection from a photoexcited dye into the conduction band of TiO_2 and subsequently dye regeneration and hole transportation to the counter electrode. An impressive solar-to-electricity power conversion efficiency of 10.4% was achieved with a panchromatic dye, when used in conjunction with conventional nonaqueous electrolytes that contain the triiodide/iodide couple.[8] One of the main problems of this device during long-term operation lies in the difficult encapsulation of volatile solvents, especially for DSCs with a plastic matrix. Thus, replacing an organic solvent-based liquid electrolyte with a solid-state hole conductor,[9,10] *p*-type semiconductor,[11,12] and solvent-free polymer electrolyte[13−15] was attempted to develop all-solid-state DSCs; however, to date, no satisfactory conversion efficiencies have been achieved in all of these cases.

Room-temperature ionic liquids (RTILs) that have good chemical and thermal stability, negligible vapor pressure, nonflammability, high ionic conductivity, and a wide electrochemical window have been intensively pursued as alternative electrolytes for DSCs[16−22] and other electrochemical devices.[23−28] However, the conversion yields obtained with ionic liquids at a full air mass (AM 1.5) solar irradiance have been markedly lower than those achieved with organic solvent-based electrolytes. Only recently were efficiencies of 5%∼6% achieved for DSCs with pure ionic liquid electrolytes.[21,22] In this paper, an ionic liquid electrolyte that consisted of 1-methyl-3-propylimidazolium iodide (PMII), 1-methyl-3-ethylimidazolium dicyanamides (EMIDCN),[29] and lithium iodide (LiI) was combined with an amphiphilic light harvester, Z-907 [Ru(H_2dcbpy)(dnbpy)$(NCS)_2$, where H_2dcbpy is 4,4′-dicarboxylic acid-2,2′-bipyridine and dnbpy is 4,4′-dinonyl-2,2′-bipyridine], to obtain a device with a solar-to-electricity efficiency of 6.6% at an irradiance of air mass of 1.5 (AM 1.5, 100 mW cm^{-2}) and >7% at lower light intensities.

Experimental Section

Reagents and Electrolytes. LiI, lithium bis(trifluoromethanesulfonyl)amide (LiTFSI), and ferrocene were purchased from Fluka (Switzerland) and used as received. 3-Methoxypropionitrile (Fluka) was distilled before use. *N*-Methylbenzimidazole (NMBI) was purchased from Aldrich (Switzerland) and recrystallized from diethyl ether. The amphiphilic Z-907 dye and standard N-719 dye [*cis*-Ru$(Hdcbpy)_2(NCS)_2(TBA)_2$, where TBA is tetra-*n*-butylammonium] were synthesized as described in our previous papers.[30,31] Ionic liquids [PMII, EMIDCN, and 1-ethyl-3-methylimidazolium bis(trifluoromethanesulfonyl)amide (EMITFSI)] were prepared according to the literature methods[29,32] and confirmed by ^{1}H NMR spectra. The molecular structures of sensitizers (Z-907, N-719) and ionic liquids (PMII, EMIDCN) are shown in Figure 1. The compositions of electrolytes used in this study are as follows. Electrolyte A was composed of 0.1 M iodine and 0.45 M NMBI in a mixture of PMII and EMIDCN (volume ratio of 13:7), whereas electrolyte B was composed of 0.1 M iodine, 0.1 M LiI, and 0.45 M NMBI in a mixture of PMII and EMIDCN (volume ratio of 13:7). The added iodine will react with the excess iodide to form triiodide.

Preparation of Double-Layer TiO_2 Electrode. The fluorine-doped SnO_2 conducting glass was first cleaned in Triton X-100 aqueous solution, washed with ethanol, and treated with 50 mM $TiCl_4$ aqueous solution at 70 °C for 30 min, to make a good mechanical contact between the following printed TiO_2 layer

* Authors to whom correspondence should be addressed. E-mail: shaik.zakeer@epfl.ch, michael.graetzel@epfl.ch.

10.1021/jp0355399 CCC: $25.00
Published on Web 11/06/2003

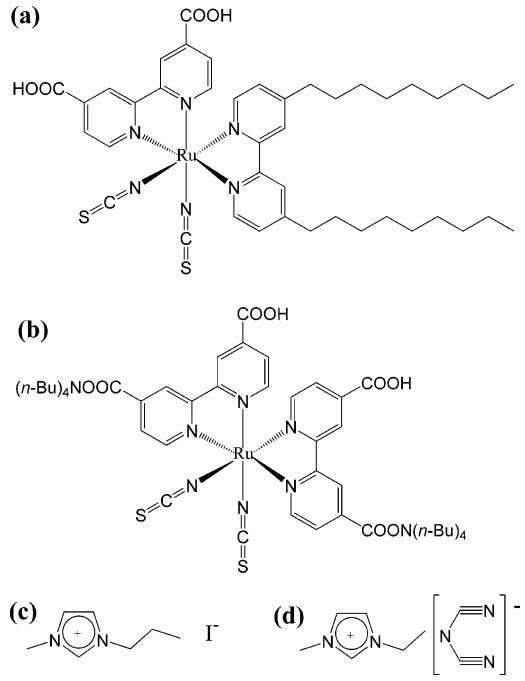

Figure 1. Molecular structures of (a) Z-907, (b) N-719, (c) PMII, and (d) EMIDCN.

and the conducting glass matrix. A 10 μm-thick film of TiO_2 particles 20 nm in size was then printed on the treated conducting glass and further coated by a 4-μm-thick second layer of 400-nm-light-scattering anatase particles (CCIC, Japan). For the second layer, the screen-printing paste is composed of 10 g of TiO_2 scattering particles 400 nm in size and 2 g of fine TiO_2 particles (15 nm in size) to obtain a mechanically tough layer. The screen-printed layer was gradually heated to 500 °C in an oxygen atmosphere and subsequently sintered at that temperature for 10 min. The layer thickness was determined using an Alpha-step 200 surface profilometer (Tencor Instruments, USA). After the assembly was treated with 40 mM $TiCl_4$ again, the layer was rinsed with water and ethanol.

Fabrication of Dye-Sensitized Solar Cells. After sintering at 500 °C and cooling to 80 °C, the double-layer structured TiO_2 electrode was dye-coated by immersion into a 0.3 mM solution of Z-907 or N-719 in acetonitrile and *tert*-butyl alcohol (volume ratio of 1:1) at room temperature for 12 h and then assembled with thermally platinized conducting glass electrodes. The electrodes were separated by a 35-μm-thick Bynel hot-melt ring (DuPont, USA) and sealed by heating. The internal space was filled with electrolytes, using a vacuum pump, to produce device A, which is composed of Z-907 dye and electrolyte A. Devices B and C contain electrolyte B with Z-907 dye and N-719 dye, respectively. The electrolyte-injection hole that was made with a sand-blasting drill on the counter electrode glass substrate was sealed with a Bynel sheet and a thin glass cover by heating. The sealed cells were aged under indoor light for 5 h before photoelectrochemical measurements.

Electrochemical Measurements. Voltammetric data were recorded at room temperature on an Autolab P20 electrochemical workstation (Eco Chimie, The Netherlands). The internal space of cells described previously was filled with ionic liquid EMITFSI, which contained 20 mM ferrocene as an internal reference compound and 0.1 M LiTFSI. The resulting thin-layer electrochemical cell was used to study the redox behavior of Z-907 dye that was anchored on interconnected TiO_2 nanocrystals. The redox potential values versus ferrocene were converted to those versus a normal hydrogen electrode (NHE) by adding a constant of 0.67 V.[33] A two-electrode electrochemical cell, which consisted of a platinum ultramicroelectrode with a radius of 5.0 μm (Bioanalytical Systems, Inc., USA) as working electrode and a platinum foil as a counter electrode, was used for the diffusion coefficient measurements of triiodide in electrolytes A and B.

Photoelectrochemical Measurements. A 450 W xenon light source (Oriel, USA) was used to give an irradiance of 100 mW cm^{-2} (the equivalent of one sun at AM 1.5) at the surface of solar cells. The spectral output of the lamp was matched in the region of 350−750 nm with the aid of a Schott K113 Tempax sunlight filter (Präzisions Glas and Optik GmbH, Germany), to reduce the mismatch between the simulated and true solar spectra to <2%. Various incident-light intensities were regulated with neutral wire mesh attenuators. The current−voltage characteristics of the cell under these conditions were obtained by applying an external potential bias to the cell and measuring the generated photocurrent with a Keithley model 2400 digital source meter (Keithley, USA). This process was fully automated using Wavemetrics software (http://www.wavemetrics.com/). A similar data acquisition system was used to control the incident photon-to-current conversion efficiency (IPCE) measurement. Under full computer control, light from a 300 W xenon lamp (ILC Technology, USA) was focused through a Gemini-180 double monochromator (Jobin Yvon Ltd., UK) onto the photovoltaic cell that was being tested. The monochromator was incremented through the visible spectrum to generate the IPCE-(λ), as defined below.

$$\mathrm{IPCE}(\lambda) = 12400\left(\frac{J_{sc}}{\lambda\phi}\right) \qquad (1)$$

where λ is the wavelength, J_{sc} the short-circuit current photocurrent (in units of mA cm^{-2}), and ϕ the incident radiative flux (in units of mW cm^{-2}).

Laser Transient Absorbance Measurements. Transparent TiO_2 mesoporous layers (8 μm thick) that had been deposited on flint glass sensitized with Z-907 were used for transient absorbance measurements. Nanosecond pulsed laser excitation was applied, using a GWU-355 broadband optical parametric oscillator pumped with a Continuum Powerlite 7030 frequency-tripled Q-switched Nd:YAG laser. The oscillator output (repetition rate of 30 Hz, pulse width at half-height of 5 ns) was tuned at a wavelength of 495 or 510 nm and attenuated by filters. To irradiate a large cross section of the sample, it was kept at a 30° angle to the excitation beam and the beam was expanded by a planoconcave lens. Laser fluence on the sample was kept at a very low level (30 μJ cm^{-2} per pulse), to ensure that, on average, less than one electron is injected per nanocrystalline TiO_2 particle upon pulsed irradiation. The probe light from a continuous-wave xenon arc lamp was passed through a first monochromator, various optical elements, the sample, and a second monochromator before being detected by a fast photomultiplier tube. Transient absorbance measurements of the oxidized-state dye were performed at a probe wavelength of 630 nm. Ground-state bleaching was monitored at a wavelength of 530 nm.

Results and Discussion

Efficient sensitization of TiO_2 nanocrystalline electrodes to visible light relies on the fact that the excited state of a dye is a stronger reductant than that in the ground state. Knowledge of the formal redox potential of the excited state ($\phi^0(S^+/S^*)$) of a dye, relative to the energy level of the TiO_2 semiconductor,

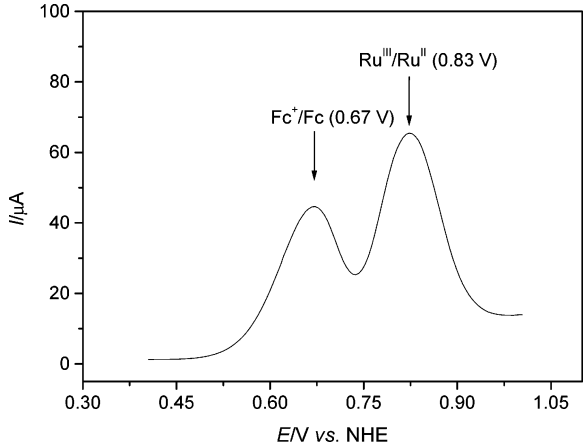

Figure 2. Square-wave voltammogram of the Z-907 dye anchored on the surface of interconnected TiO_2 nanocrystals. Potential step increment, 5 mV; amplitude, 20 mV; frequency, 10 Hz; scan rate, 50 mV s^{-1}.

allows a priori determination of the direction of current flow. An approximate value of $\phi^0(S^+/S^*)$ of a dye can be extracted from the formal potential of the ground state [$\phi^0(S^+/S)$] and its excitation energy (E_{0-0}), according to eq 2:[34,35]

$$\phi^0(S^+/S^*) = \phi^0(S^+/S) - \frac{E_{0-0}}{F} \qquad (2)$$

where F is the Faraday constant. Quasi-reversible electrochemical behavior of polypyridyl ruthenium complexes anchored on mesoporous TiO_2 film has been studied with a conventional three-electrode electrochemical cell by cyclic voltammetry.[36] In the present work, a thin-layer electrochemical cell composed of a Z-907-sensitized TiO_2 nanocrystalline electrode as the working electrode and a platinized conducting glass as the counter electrode was used to study the redox property of the sensitizer. Because of the steady-state behavior of normal linear sweep voltammograms of a thin-layer electrochemical cell,[37] square wave voltammetry[38−41] with inherently high analytical sensitivity and strong immunity to capacitive effects was used to obtain accurate $\phi^0(S^+/S)$ values of the Z-907 dye. As shown in Figure 2, a well-defined redox wave is observed for the Ru^{III}/Ru^{II} couple (+0.83 V vs NHE). The wave centered at +0.67 V is ascribed to the direct electron transfer between ferrocene (20 mM) and the conducting glass electrode. Because the equilibrium potentials of electrolytes A and B (derived approximately by the Nernst expression[42]) are 0.463 and 0.461 V vs NHE, respectively, there will be a large thermodynamic driving force for regeneration of the Z-907 dye by iodide in these electrolytes. The E_{0-0} value was estimated to be 1.64 eV by the method reported in our previous paper.[31] Thus, the $\phi^0(S^+/S^*)$ of the Z-907 dye is derived to be −0.82 V vs NHE by eq 2 and is comparable to that reported for the N3 dye [$Ru(H_2dcbpy)_2(NCS)_2$], which was confirmed to be an efficient sensitizer of DSCs. The detailed comparisons of absorption, luminescence, and redox properties of amphiphilic ruthenium(II) dyes and the standard N3 dye in solutions have been described in our previous paper.[43]

Photocurrent action spectra are shown in Figure 3. The maximum IPCE values at 550 nm are 66% and 76% for devices A and B, respectively. Figure 4 presents the photocurrent density−voltage curves for devices A−C at an AM 1.5 irradiance of 100 mW cm^{-2}, and the device efficiencies at different light intensities are listed in Table 1. The short-circuit

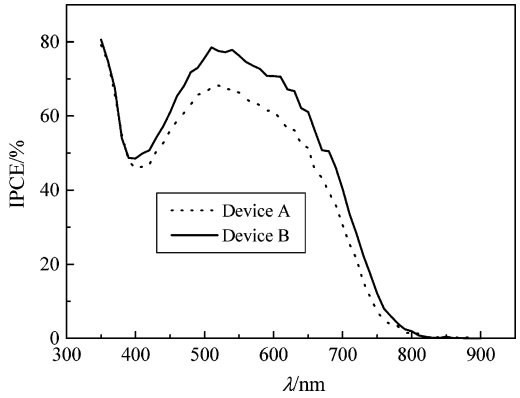

Figure 3. Photocurrent action spectra for devices A and B. Cell active area is 0.152 cm^2.

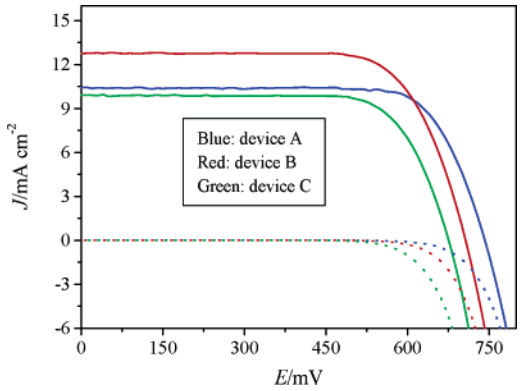

Figure 4. Current density−voltage characteristics of devices A−C at AM 1.5 (100 mW cm^{-2}) illumination (solid curves) and in darkness (dotted curves). Cell active area is 0.152 cm^2.

TABLE 1: Device Efficiency (η) at Different Light Intensities

	η at different incident light intensities (%)[a]			
device	0.01 sun	0.1 sun	0.5 sun	1.0 sun
A	6.2	6.6	6.3	5.7
B	7.2	7.2	7.1	6.6
C	5.3	5.3	5.3	5.0

[a] The spectral distribution of the lamp mimics air mass (AM) 1.5 solar light. The term 1.0 sun corresponds to an intensity of 100 mW cm^{-2}. The efficiencies reported here are the average data of four cells with a deviation of ±0.2.

current photocurrent (J_{sc}), open-circuit voltage (V_{oc}), and fill factor (FF) of device A without lithium salt in its electrolyte are 10.4 mA cm^{-2}, 742 mV, and 0.740, respectively, yielding an overall power conversion efficiency (η) of 5.7%. For device B, which has 0.1 M LiI in its electrolyte, the corresponding device parameters (J_{sc}, V_{oc}, FF, and η) are 12.8 mA/cm^2, 707 mV, 0.727, and 6.6%, respectively. This is the first time such a high efficiency was obtained for DSCs with pure ionic liquid electrolytes under full sunlight. As shown in Figure 5, the addition of 0.1 M LiI to electrolyte A does not influence the limiting current of cathodic reduction of triiodide but efficiently improves the value of J_{sc} (device B). This clearly indicates that the relatively low J_{sc} value of device A is not limited by the slow diffusion of triiodide in electrolyte A. The apparent diffusion coefficient of triiodide in electrolytes A and B was derived to be 4.4×10^{-7} cm^2 s^{-1}, which is 2.3 times greater than that in pure PMII,[22] because of the lower dynamic viscosity of EMIDCN, compared with PMII.[29] Indeed, the substitution of LiI in device B by the same concentration of LiTFSI produced

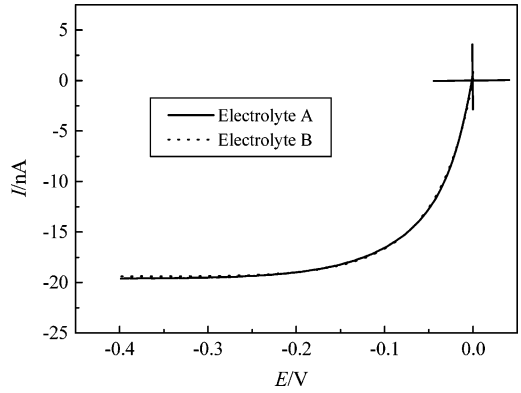

Figure 5. Steady-state voltammograms of electrolytes A and B with a platinum ultramicroelectrode. Scan rate is 10 mV s^{-1}.

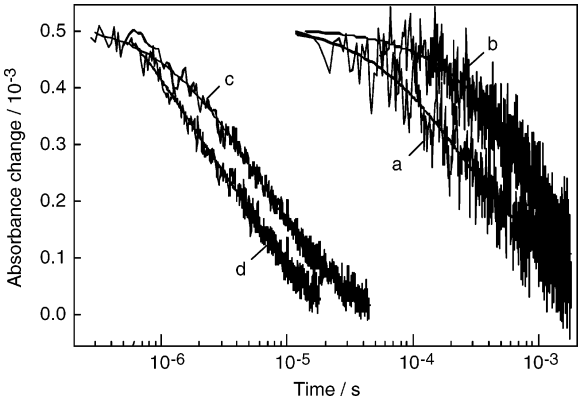

Figure 6. Transient absorption data following the decay of oxidized state of Z-907 adsorbed on a transparent TiO_2 nanocrystalline film. Decay of the dye cation was monitored in various liquids: (a) pure EMIDCN, (b) EMIDCN with 0.1 M LiTFSI, (c) electrolyte A, and (d) electrolyte B. Data were collected under open-circuit conditions at a probe wavelength of 630 nm, using 510-nm laser excitation. Oscillograms shown were averaged over 4096 shots and normalized to an initial ΔA value of 5×10^{-4}.

a device with almost identical J_{sc} and V_{oc} values, confirming that the enhanced performance of device B, compared with device A, was mainly caused by the Li^+ ion, rather than by a small increase in the concentration of iodide. Although in darkness, the V_{oc} value of DSCs is zero, upon illumination, electron injection from the excited dye into the TiO_2 leads to the quasi-Fermi level splitting that is the origin of the photovoltage of DSCs.[44] Because of the negligible difference (2 mV) in equilibrium potentials of electrolytes A and B, the 35 mV difference in the V_{oc} values of devices A and B should be ascribed to the difference in the flat-band potential (ϕ_{fb}) of nanostructured TiO_2 films that can be controlled by the specific adsorption of Li^+ cations. In addition, compared to device B, device C (prepared with the standard N-719 dye and electrolyte B) showed lower total conversion efficiencies, because of the enhanced back transfer of injected electrons from the conduction band of the TiO_2 film to the triiodide. The undesirable back electron transfer is also responsible for the lower V_{oc} value (675 mV). Obviously, the use of an amphiphilic dye, Z-907, markedly suppressed this problem. The most likely reason for the suppression of the back electron reaction is that the long hydrocarbon chains of the Z-907 dye interacts laterally to form an aliphatic network, thereby increasing the distance between the triiodide and electrons trapped on the TiO_2 surface and thus hindering the back-electron-transfer process. This has been indicated by the dark current measurements shown in Figure 4.

Laser flash photolysis experiments were performed to understand the action mode of the Li^+ ion in enhancing the power conversion efficiency of the aforementioned devices. The concentration of oxidized-state dye molecules produced upon electron injection into the conduction band of the TiO_2 film is directly monitored with nanosecond transient absorbance measurements. In Figure 6, the decay of absorption signal (curves a and b) in pure EMIDCN is attributed to the recombination between electrons trapped in the mesoporous TiO_2 film and the oxidized-state dye. In the presence of electrolytes, signal decay (curves c and d) is essentially due to the reduction of oxidized-state dye molecules by iodide. The pulsed laser intensity was kept at a very low level, to ensure that less than one charge-separated pair (injected electron/dye cation) was produced, on average, per TiO_2 particle. Although measurements were performed without the application of an external bias, such a condition is still believed to be similar to that which prevails for the photovoltaic device that is functioning under natural sunlight. Figure 6 shows that interception of the oxidized-state dye by iodide (dye regeneration) competes efficiently with the recombination process. The addition of Li^+ ions caused the half-reaction time ($t_{1/2}$) for recombination to increase typically from 0.2 ms to 0.8 ms. Dye regeneration in the presence of iodide was observed, in all cases, to be virtually complete after 50 μs, whereas charge recombination was practically negligible within the same time frame.[45,46] On the other hand, the presence of Li^+ ions accelerated the dye regeneration, with $t_{1/2}$ decreasing from 6 μs to 3 μs. A somewhat stronger effect of the Li^+ cations in the dye regeneration rate ($\sim$3$-$4 times) by iodide was observed in conventional solvents, which was attributed to electrostatic interactions.[47] In ionic liquid electrolytes, such interactions are expected to be weaker, because of the high ionic strength, which screens the surface charge that is due to any lithium adsorption onto the surface. Hence, the effect of Li^+ ions on the kinetics of dye regeneration by iodide cannot fully rationalize an increase in the power conversion efficiency of device B.

The enhancement in device efficiencies may be attributed to an improved electron injection from the excited-state dye into the conduction band of the oxide. Direct determination of the absolute injection quantum yield (Φ_i) can be achieved by monitoring the ground-state bleaching signal of sensitizers upon nanosecond laser flash photolysis.[48] At 530 nm, absorption by the conduction-band electrons and the excited and oxidized states of the sensitizer is negligible.[49] Thus, the transient absorption signal measured at this probe wavelength is mainly due to the bleaching and repopulation of the ground state of the dye. Photoexcited dye molecules that do not inject electrons into TiO_2 are deactivated to their ground-state within 10 ns. On the other hand, dye cations produced by the photoinduced electron-transfer process recapture the injected electron only in the microsecond-millisecond time domain. These two reaction channels are easily discriminated by the large difference in rate constants. Because the laser pulse duration (5 ns) is shorter than the time constant of the fastest deactivation process ($\sim$10 ns), the amplitude of the signal bleaching measured at the end of the laser excitation is proportional to the initial concentration of produced excited states. Quantitative evaluation of the amplitude of the fast and slow kinetic components of the ground-state repopulation allow direct assessment of the proportion of dye excited states decaying through natural deactivation and charge injection, respectively. Figure 7 shows that, in the presence of Li^+ ions, a fast recovery of the ground-state population was not observed, meaning that the injection quantum

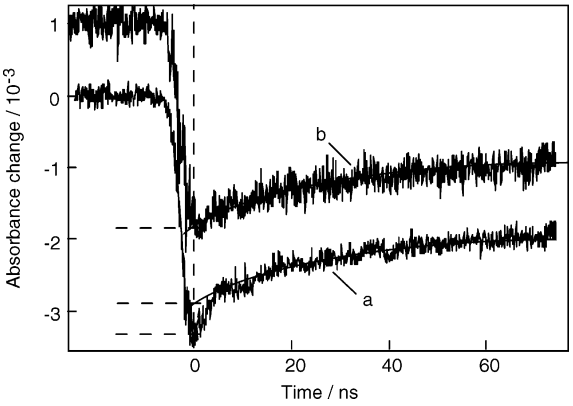

Figure 7. Transient absorption changes observed at $\lambda = 530$ nm upon nanosecond laser excitation of a Z-907 dye-sensitized nanocrystalline TiO_2 film in (a) electrolyte A and (b) electrolyte B. The absolute injection quantum yield is obtained from both ground-state bleaching signals as the ratio of the absorbance change at a longer time scale (20 ns $< t >$ 80 ns), extrapolated to time zero, over the initial absorbance decrease observed upon laser excitation of the dye. Curve b is shifted vertically by 1 mOD for clarity.

yield Φ_i was similar to unity. Without the addition of Li^+ ions, the amplitudes of the fast and slow kinetic components were determined as being ~10% and ~90% of the initial bleaching signal, respectively, yielding only $\Phi_i = 0.90$.

Specific adsorption of small cations onto oxide semiconductors is known to possibly modify surface charge, band-edge positions, and the energy-level distribution of surface states.[50] The flat-band potential of the semiconductor in a dry aprotic electrolyte can be shifted to considerably more positive values upon the adsorption of potential-determining ions such as the Li^+ ion.[45] Such an improvement of the driving force for electron injection by several hundred millielectronvolts is expected to increase the rate and yield of the primary charge separation process considerably.[48,51] With another Ru(II) complex as a sensitizer, Meyer et al.[52] indeed showed that the adsorption of Li^+ cations onto the surface of TiO_2 increases the quantum yield of electron injection with no apparent influence on the rate of the back electron transfer. In our case, a similar effect is likely to be the primary cause of the 16% efficiency difference between devices A and B.

Conclusions

In summary, a thin-layer electrochemical cell has been conveniently used to study the redox potential of sensitizers that are anchored on a mesoporous film, in conjunction with square-wave voltammetry. For the first time in dye-sensitized nanocrystalline solar cells with pure ionic liquid electrolytes, an efficiency of 6.6% was obtained at an illumination of air mass (AM 1.5) sunlight. The addition of lithium iodide to pure ionic liquid electrolyte significantly enhances the efficiency, because of an increase in the electron injection yield and dye regeneration rate. The present findings should foster widespread application of flexible dye-sensitized solar cells.

Acknowledgment. We are grateful to T. Koyanagi (CCIC, Japan) for providing the 400-nm TiO_2 particles, P. Comte for TiO_2 film fabrication, and Dr. R. Humphry-Baker for helpful discussion. The Swiss Science Foundation, Swiss Federal Office for Energy (OFEN), and the European Office of the U.S. Air Force (under Contract No. F61775-00-C0003) have supported this work.

References and Notes

(1) Turner, J. A. *Science* **1999**, *285*, 687−689.
(2) Shah, A.; Torres, P.; Tscharner, R.; Wyrsch, N.; Keppner, H. *Science* **1999**, *285*, 692−698.
(3) Dresselhaus, M. S.; Thomas, I. L. *Nature* **2001**, *414*, 332−337.
(4) O'Regan, B.; Grätzel, M. *Nature* **1991**, *353*, 737−740.
(5) Hagfeldt, A.; Grätzel, M. *Chem. Rev.* **1995**, *95*, 49−68.
(6) Hagfeldt, A.; Grätzel, M. *Acc. Chem. Res*. **2000**, *33*, 269−277.
(7) Grätzel, M. *Nature* **2001**, *414*, 338−344.
(8) Nazeeruddin, M. K.; Péchy, P.; Renouard, T.; Zakeeruddin, S. M.; Humphry-Baker, R.; Comte, P.; Liska, P.; Cevey, L.; Costa, E.; Shklover, V.; Spiccia, L.; Beacon, G. B.; Bignozzi, C. A.; Grätzel, M. *J. Am. Chem. Soc*. **2001**, *123*, 1613−1624.
(9) Bach, U.; Lupo, D.; Comte, P.; Moser, J. E.; Weissortel, F.; Salbeck, J.; Spreitzer, H.; Grätzel, M. *Nature* **1998**, *395*, 583−586.
(10) Krüger, J.; Plass, R.; Grätzel, M.; Matthieu, H. J. *Appl. Phys. Lett.* **2002**, *81*, 367−369.
(11) Kumara, G. R. A.; Kaneko, S.; Okuya, M.; Tennakone, K. *Langmuir* **2002**, *18*, 10493−10495.
(12) O'Regan, B.; Lenzmann, F.; Muis, R.; Wienke, J. *Chem. Mater*. **2002**, *14*, 5023−5029.
(13) Nogueira, A. F.; Durrant, J. R.; DePaoli, M. A. *Adv. Mater*. **2001**, *13*, 826−830.
(14) Stathatos, E.; Lianos, P.; Lavrencic-Stangar, U.; Orel, B. *Adv. Mater*. **2002**, *14*, 354−357.
(15) Stergiopoulos, T.; Arabatzis, I. M.; Katsaros, G.; Falaras, P. *Nano Lett*. **2002**, *2*, 1259−1261.
(16) Papageorgiou, N.; Athanassov, Y.; Armand, M.; Bonhôte, P.; Pettersson, H.; Azam, A.; Grätzel, M. *J. Electrochem. Soc*. **1996**, *143*, 3099−3108.
(17) Matsumoto, H.; Matsuda, T.; Tsuda, T.; Hagiwara, R.; Ito, Y.; Miyazaki, Y. *Chem. Lett*. **2001**, 26−27.
(18) Kubo, W.; Makimoto, Y.; Kitamura, T.; Wada, Y.; Yanagida, S. *Chem. Lett*. **2002**, 948−949.
(19) Kubo, W.; Kitamura, T.; Hanabusa, K.; Wada, Y.; Yanagida, S. *Chem. Commun*. **2002**, 374−375.
(20) Kubo, W.; Kambe, S.; Nakade, S.; Kitamura, T.; Hanabusa, K.; Wada, Y.; Yanagida, S. *J. Phys. Chem. B* **2003**, *107*, 4374−4381.
(21) Wang, P.; Zakeeruddin, S. M.; Exnar, I.; Grätzel, M. *Chem. Commun*. **2002**, 2972−2973.
(22) Wang, P.; Zakeeruddin, S. M.; Comte, P.; Exnar, I.; Grätzel, M. *J. Am. Chem. Soc*. **2003**, *125*, 1166−1167.
(23) Fuller, J.; Breda, A. C.; Carlin, R. T. *J. Electrochem. Soc*. **1997**, *144*, L67−L70.
(24) McEwen, A. B.; Ngo, H. L.; LeCompte, K.; Goldman, J. L. *J. Electrochem. Soc*. **1999**, *146*, 1687−1695.
(25) Wasserscheid, P.; Keim, W. *Angew. Chem., Int. Ed*. **2000**, *39*, 3773−3789.
(26) Naudin, E.; Ho, H. A.; Branchaud, S.; Breau, L.; Belanger, D. *J. Phys. Chem. B* **2002**, *106*, 10585−10593.
(27) Sutto, T. E.; De Long, H. C.; Trulove, P. C. *Z. Naturforsch. A: Phys. Sci*. **2002**, *57*, 839−846.
(28) Lu, W.; Fadeev, A. G.; Qi, B.; Smela, E.; Mattes, B. R.; Ding, J.; Spinks, G. M.; Mazurkiewicz, J.; Zhou, D.; Wallace, G. G.; MacFarlane, D. R.; Forsyth, S. A.; Forsyth, M. *Science* **2002**, *297*, 983−987.
(29) MacFarlane, D. R.; Golding, J.; Forsyth, S.; Forsyth, M.; Deacon, G. B. *Chem. Commun.* **2001**, 1430−1431.
(30) Wang, P.; Zakeeruddin, S. M.; Moser, J. E.; Nazeeruddin, M. K.; Sekiguchi, T.; Grätzel, M. *Nature Mater.* **2003**, *2*, 402−407.
(31) Nazeeruddin, M. K.; Kay, A.; Rodicio, I.; Humphry-Baker, R.; Müller, E.; Liska, P.; Vlachopoulos, N.; Grätzel, M. *J. Am. Chem. Soc*. **1993**, *115*, 6382−6390.
(32) Bonhôte, P.; Dias, A. P.; Armand, M.; Papageorgiou, N.; Kalyanasundaram, K.; Grätzel, M. *Inorg. Chem*. **1996**, *35*, 1168−1178.
(33) Lai, R. Y.; Bard, A. J. *J. Phys. Chem. B* **2003**, *107*, 5036−5042.
(34) Qu, P.; Meyer, G. J. In *Electron Transfer in Chemistry*; Balzani, V., Ed.; Wiley: Weinheim, Germany, 2001; Vol. IV, pp 353−411.
(35) Grätzel, M.; Moser, J.-E. In *Electron Transfer in Chemistry*; Balzani, V., Ed.; Wiley: Weinheim, Germany, 2001; Vol. V, pp 589−644.
(36) Heimer, T. A.; D'Arcangelis, S. T.; Farzad, F.; Stipkala, J. M.; Meyer, G. J. *Inorg. Chem*. **1996**, *35*, 5319−5324.
(37) Hubbard, A. T.; Anson, F. C. In *Electroanalytical Chemistry*; Bard, A. J., Ed.; Marcel Dekker: New York, 1970; Vol. 4, pp 129−214.
(38) Osteryoung, J.; O'Dea, J. J. In *Electroanalytical Chemistry*; Bard, A. J., Ed.; Marcel Dekker: New York, 1986; Vol. 14, pp 209−308.
(39) Kumar, V.; Heineman, W. R. *Anal. Chem*. **1987**, *59*, 842−846.
(40) Aoki, K.; Osteryoung, J. *J. Electroanal. Chem*. **1988**, *240*, 45−51.
(41) Osteryoung, J. *Acc. Chem. Res*. **1993**, *26*, 77−83.

(42) Bard, A. J.; Faulkner, L. R. *Electrochemical Methods: Fundamentals and Applications*, 2nd ed.; Wiley: Weinheim, Germany, 2001.
(43) Zakeeruddin, S. M.; Nazeeruddin, M. K.; Humphry-Baker, R.; Péchy, P.; Quagliotto, P.; Barolo, C.; Viscard, G.; Grätzel, M. *Langmuir* **2002**, *18*, 952−954.
(44) Cahen, D.; Grätzel, M.; Guillemoles, J. F.; Hodes, G. In *Electrochemistry of Nanomaterials*; Hodes, G., Ed.; Wiley: Weinheim, Germany, 2001; pp 201−229.
(45) Haque, S. A.; Tachibana, Y.; Willis, R. L.; Moser, J. E.; Grätzel, M.; Klug, D. R.; Durrant, J. R. *J. Phys. Chem. B* **2000**, *104*, 538−547.
(46) Willis, R. L.; Olson, C.; O'Regan, B.; Lutz, T.; Nelson, J.; Durrant, J. R. *J. Phys. Chem. B* **2002**, *106*, 7605−7613.
(47) Pelet, S.; Moser, J. E.; Grätzel, M. *J. Phys. Chem. B* **2000**, *104*, 1791−1795.
(48) Moser, J. E.; Wolf, M.; Lenzmann, F.; Grätzel, M. *Z. Phys. Chem.* **1999**, *212*, 85−92.
(49) Moser, J. E.; Noukakis, D.; Bach, U.; Tachibana, Y.; Klug, D. R.; Durrant, J. R.; Humphry-Baker, R.; Grätzel, M. *J. Phys. Chem. B* **1998**, *102*, 3649−3650.
(50) Heller, A. *Acc. Chem. Res.* **1981**, *14*, 154−162.
(51) Tachibana, Y.; Haque, S. A.; Mercer, I. P.; Moser, J. E.; Klug, D. R.; Durrant, J. R. *J. Phys. Chem. B* **2001**, *105*, 7424−743.
(52) Kelly, C. A.; Farzad, F.; Thompson, D. W.; Stipkala, J. M.; Meyer, G. J. *Langmuir* **1999**, *15*, 7047−7054.